JOURNAL OF APPLIED ELECTROCHEMISTRY 23 (1993) 1181–1186

A phenomenological approach to ionic mass transfer at rotating disc electrodes with a hanging column of electrolyte solution

C.I. ELSNER, P.L. SCHILARDI, S.L. MARCHIANO

Instituto de Investigaciones Fisicoquímicas Teóricas y Aplicadas (INIFTA), Facultad de Ciencias Exactas, Universidad Nacional de La Plata, Sucursal 4, Casilla de Correo 16, (1900) La Plata, Argentina

Received 18 November 1992; revised 6 April 1993

Experimental data for the behaviour of a rotating disc electrode with a hanging electrolyte column of varying height are presented. A correlation involving the limiting current density, the rotation speed, and the physicochemical properties of the solution is established. The macroscopic effective copper electrodeposit thickness distribution is determined. Results obtained for different electrode designs are discussed in terms of an additional flow of reactant, and an apparent change in the effective electrode area caused by liquid column contraction. From the results the most suitable experimental conditions for the application of the rotating disc electrode with a hanging column of electrolyte to electrochemical kinetic studies can be found.

1. Introduction

Since the description of the rotating disc electrode (rde) by Levich in 1942 [1–3], various designs of this type of electrode have been used in electrochemical kinetic studies [4–9]. However, occasionally border effects, partial or complete blockage of the electrode surface, roughness effect and bubble formation [10, 11], highlight the need for new designs for rotating electrode devices as reported in the literature [12, 13]. One such variant is the rotating disc electrode with a hanging column of electrolyte (rdehc) which has been used for the study of metal corrosion [14, 15] and other electrochemical reactions on relatively soft metals to avoid possible mechanical stresses produced when the specimen is encased in insulating materials. As already known for the conventional rde, in this case the limiting current is related to the square root of the electrode rotation speed. This fact means that the Levich equation for the rde is directly applicable to the rdehc device; however, for this device the hydrodynamic boundary layer conditions are different from those of rde [1–3]. For the rdehc it is expected that the ionic mass transfer is influenced by the complex streamlines inside the cylindrical liquid volume extending from the solution free surface plane to the electrode surface. As a first approach the hydrodynamics of the rdehc can be approximated to that of a fluid within a confined cylindrical box under axial rotation [16, 17]. Accordingly, two distinguishable flow regimes are produced in the cylindrical fluid box, namely a primary flow which corresponds to the angular fluid velocity component, and a secondary flow due to the axial and radial fluid velocity components. Therefore, for this type of electrode arrangement complicated hydrodynamic and diffusional profiles are produced. However, within the laminar flow regime the ionic mass transport limiting current depends on the square root of ω, the rotation speed of the working electrode [13]. This is, in principle, an interesting fact which justifies the application of this type of rotating disc electrode design for the investigation of electrochemical reactions such as corrosion and passivation processes at soft conducting surfaces.

The present work discusses specific aspects of ionic mass transfer to rdehc's and indicates the conditions in which this type of electrode approaches the behaviour of a conventional rde. The present results also offer the possibility of establishing the optimal design and working conditions imposed by experimental test.

2. Experimental details

The electrochemical cell consisted of a single cylindrical compartment of about 0.5 dm^3 capacity provided with a rde. The rde was placed onto the electrolyte surface and then raised to a height, h_m. In this way an electrolyte column was formed (Fig. 1(a)). Different electrodes made of either nickel (0.2 cm $\leqslant d_e \leqslant$ 1.4 cm) or copper (d_e = 0.8 cm), where d_e is the disc diameter, were used.

Four electrode arrangements were employed for investigating several phenomenological aspects of ionic mass transport processes at the rdehc's:

(i) Bare nickel electrodes. In this case the active area comprised the disc and the corresponding lateral cylindrical area (electrode 1).

(ii) A rde whose lateral wall was electrically insulated with a thin layer of epoxy resin (electrode 2).

(iii) A rde embedded axially into a PTFE ring

0021-891X

(thickness 5 mm) as for a conventional rde device (electrode 3).

(iv) Similar bare-type electrodes, also made of copper, with the main purpose of determining the macroscopic effective current distribution (electrode 4).

Each rdehc was coupled to a Tacussel rde circuit run in the 500 r.p.m $\leqslant \omega \leqslant$ 2500 r.p.m. range.

For the nickel rde the following test reaction was employed:

$$[Fe(CN)_6]^{3-} + e^- \rightarrow [Fe(CN)_6]^{4-} \qquad (1)$$

by using 0.02 M $K_4[Fe(CN)_6]$ + 0.02 M $K_3[Fe(CN)_6]$ + 1 M NaOH (solution A). In this case a platinum counter electrode (8 cm^2 apparent area) was employed and the working potential was measured against either a saturated calomel electrode (SCE) or a platinum electrode immersed in solution A connected to the cell through a Luggin–Haber capillary tip. In order to determine the influence of ν, the kinematic viscosity of the solution, on the rate of ionic mass transport, carboxymethyl cellulose sodium salt (CMC) was added to the solution at concentrations lower than 0.5% w/w, i.e. within a concentration range where for the range of ω covered in the present work, the Newtonian behaviour is practically fulfilled.

Ionic mass transfer to copper rdehc's was tested by using the following reaction:

$$Cu^{2+} + 2e^- \rightarrow Cu^0 \qquad (2)$$

In this case the electrical circuit was completed by a copper counter electrode (7 cm^2 apparent area). The electrolyte solution was 0.02 M $CuSO_4 \cdot 5H_2O$ + 1 M H_2SO_4 (solution B), and the reference electrode was a piece of copper dipped into the same electrolyte solution and connected to the rest of the cell as indicated above.

The electrolyte solutions were prepared from AR chemicals and twice distilled water.

The values of D, the diffusion coefficients of the reacting species, were determined using a conventional Tacussel platinum rde, and the kinematic viscosity of the solutions was measured with a Cannon–Fenske pipette. All these values were checked against the literature [18–20].

Before each run the working electrode was mechanically polished to a mirror surface with 0.3 μm grit alumina powder. The alignment and mounting of the rdehc device were carefully controlled to avoid vibration and spurious turbulence in the system. The height of the hanging liquid column (h_m) (Fig. 1(a)) was determined by using an electronic micrometer with a $\pm$0.0001 cm accuracy. The different experiments can be summarized as follows.

2.1. *Ionic mass transfer at Ni rdehc with solution A*

(i) Runs made with bare nickel electrodes (electrode 1) by changing h_m in the 0.02 cm $\leqslant h_m \leqslant$ 0.3 cm range.
(ii) Runs made with the electrically insulated lateral wall nickel rdehc's (electrodes 2 and 3), by either changing h_m as in (i), or by a direct immersion of the electrode in the solution.

In both cases, the influence of ν on the ionic mass transport rate was also determined.

2.2. *Ionic mass transfer at Cu rdehc with solution B*

The macroscopic distribution of the copper electrodeposit at rdehc was measured from photography of the working electrode resulting for different h_m values, by setting the applied potential in the limiting current range.

3. Results

3.1. *Ionic mass transfer at the Ni rdehc*

The cathodic polarization curves for Reaction 1 exhibit a typical ionic mass transfer controlled limiting current, I_L. For a nickel bare rdehc (electrode 1), I_L increases linearly with the square root of ω, the straight line going through the origin (Fig. 2). The slope of these straight lines increases as h_m is decreased.

Results obtained with a lateral insulated nickel rdehc (electrode 2), also yield linear I_L against $\omega^{1/2}$ relationships, but in this case, the following two interesting h_m-dependent effects are seen (Fig. 3). When the value of h_m is smaller than a certain critical liquid column height, h_c, the I_L against $\omega^{1/2}$ linear plot exhibits practically the slope predicted from Levich equation for the rde with an error of 10%, although in this case the straight line at $\omega = 0$ exhibits a positive ordinate. On the other hand, when $h_m > h_c$, linear I_L against $\omega^{1/2}$ plots are also observed, but intercepting the origin. The slope of these lines decreases as h_m increases, and the value of h_c lies between 0.15 and 0.21 cm.

The relationship among I_L, h_m and ω for electrodes 1 and 2 are illustrated in Figs 4 and 5 as log $I_L/\omega^{1/2}$ against log h_m. These plots for electrode 2 (Fig. 5) show a region where log $I_L/\omega^{1/2}$ becomes practically independent of log h_m, and a region where log $I_L/\omega^{1/2}$ decreases linearly with log h_m. The interception of these two straight lines determines the value of h_c for each value of d_e according to the equation:

$$h_c = 0.85\, d_e^{2/5} \qquad (3)$$

The same behaviour is observed in CMC-containing solutions in the $0.98 \times 10^{-2}\ cm^2\ s^{-1} < \nu < 2.52 \times 10^{-2}\ cm^2\ s^{-1}$ range.

The results obtained for Reaction 1 on electrode 2 can be expressed in terms of the following correlation:

$$I_L = A + 0.62 z F S D^{2/3} \nu^{-1/6} c \omega^{1/2} \qquad (4)$$

where A is a complex function of h_m, and S is the effective electrode area. The second term of Equation 4 coincides with Levich's equation for the rde.

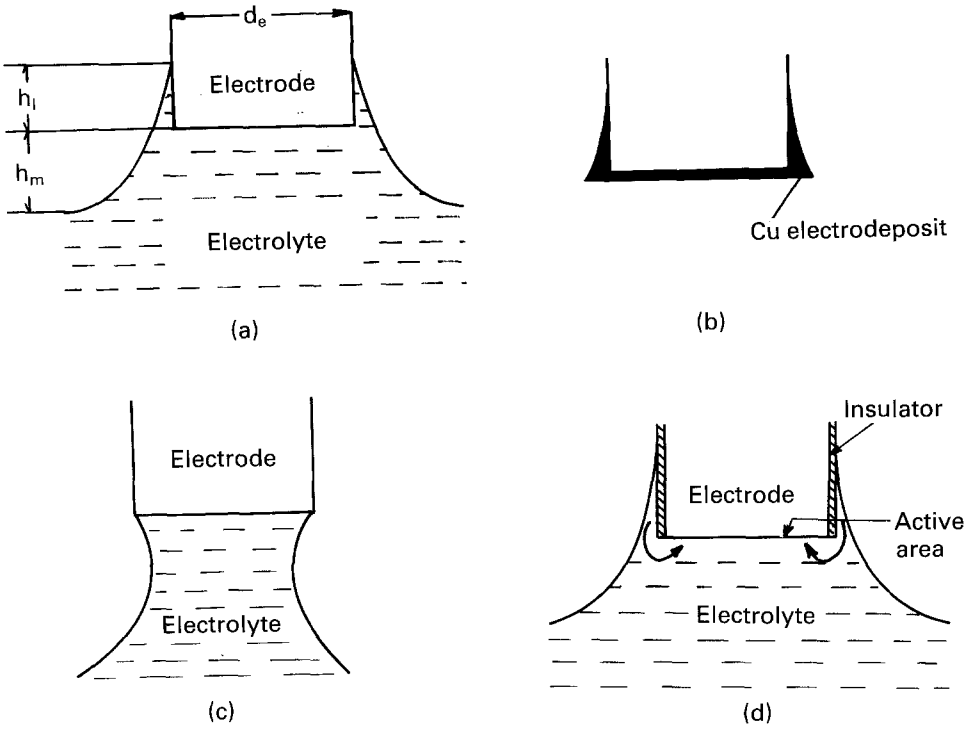

Fig. 1 (a) Scheme of the rdehc: h_m = liquid column height: h_L = height of the solution at the lateral wall of the electrode, (climbing effect) and d_e the radius of the disc; (b) scheme of the copper electrodeposit thickness distribution for $h_m < 0.1$ cm; (c) scheme of the column contraction; (d) scheme of the diffusional flow (see arrows) from the lateral climbing solution to the disc area.

3.2. *Ionic mass transfer at Cu rdehc*

The main purpose of these runs was to determine the effective current distribution at the rdehc at different constant potentials E. Runs were made at $E \leqslant 0.45$ V under constant charge condition at $\omega = 1500$ r.p.m, with h_m varied in the $0.02\,\text{cm} \leqslant h_m \leqslant 0.3\,\text{cm}$ range.

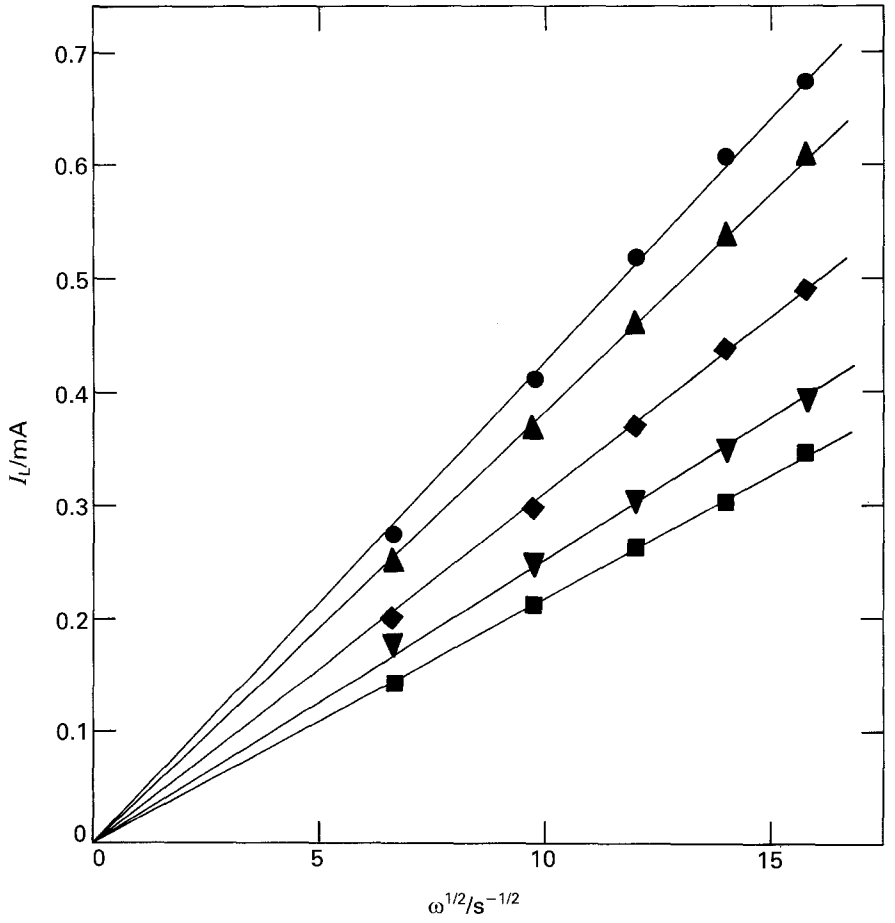

Fig. 2. Limiting current (I_L) against the square root of the rotation rate ($\omega^{1/2}$) plot for a bare nickel rde for different meniscus height. 0.02 M $K_3[Fe(CN)_6]$ + 0.02 M $K_4[Fe(CN)_6]$ + 1 M NaOH, 25 °C. Electrode disc geometric area 0.03 cm^2. Key for h_m(mm): (●) 0.387; (▲) 0.688; (◆) 0.947; (▼) 1.294 and (■) 1.579.

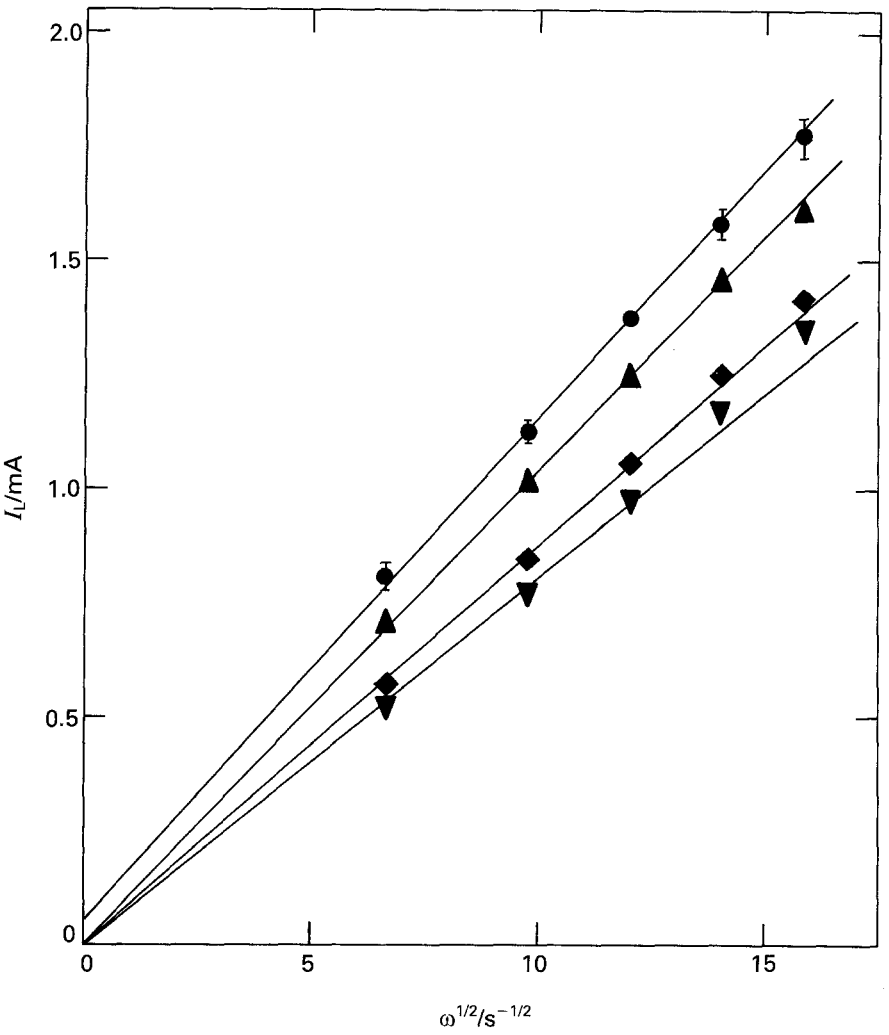

Fig. 3. Limiting current (I_L) against the square root plot of the rotation rate ($\omega^{1/2}$) for an insulated lateral wall nickel rde for different h_m. 0.02 M $K_3[Fe(CN)_6]$ + 0.02 M $K_4[Fe(CN)_6]$ + 1 M NaOH, 25 °C. Electrode disc geometric area 0.14 cm^2. Key for h_m(mm): (●) 0.237, 0.854 and 1.568; (▲) 2.018; (◆) 2.587 and (▼) 2.678.

In general, the distribution of the copper electrodeposit thickness changes with h_m as follows. For $h_m < h_c$, where h_c is related to the condition at which the I_L against $\omega^{1/2}$ linear plot intercepts the origin, the copper electrodeposit grows simultaneously on both the disc and the lateral wall up to a certain height (h_L). The value of h_L defines the lateral wetting (climbing) height. In this case the thickest copper electrodeposit appears at the border of the rdehc (Fig. 1(b)).

Otherwise, when $h_m \cong h_c$ the value of h_L becomes zero. Then, the copper electrodeposit covers homogeneously the entire disc surface. For sufficiently large values of h_m, although smaller than the meniscus rupture height (h_r), two copper electrodeposition domains on the disc surface can be distinguished, one at the centre of the disc, the other as an external concentric ring. The thickness of the copper electrodeposit at the concentric ring becomes much smaller than that at the centre of the disc. Likewise, the concentric ring to disc centre copper electrodeposit area ratio increases as h_m is increased.

4. Discussion

Results show that ionic mass transfer to rdehc's is more complicated than that to a conventional rde. For rdehc's the ionic mass transfer equation depends on whether the lateral face of the rde device is either bare or insulated.

For the bare-type of rdehc when $h_m < h_c$ there is a solution climbing effect which decreases as h_m increases. Thus, the effective electrode area is always greater than the rde area because of the lateral surface contribution. When $h_m = h_c$ the effective electrode area equals the rde area. If h_m is further increased, a new effect related to the contraction of the hanging liquid column begins to operate, leading to a gradual decrease of the effective electrode area. A scheme of this effect is depicted in Fig. 1(c). The decrease in effective electrode area is apparently reflected in the decrease of the slope of the I_L against $\omega^{1/2}$ plot.

For the insulated-type rdehc, the appearance of a finite ordinate for $\omega = 0$ when $h_m < h_c$ can be explained by considering the contribution of a diffusional flow of solution components from the solution in contact with the insulated lateral face of the electrode to the depleted solution in contact with the disc surface. A scheme of this effect is depicted in Fig. 1(d). This flow of solution components appears to be little dependent on the hydrodynamic conditions. However, when $h_m > h_c$, the additional flow of solution components disappears because only the disc surface is in contact with the solution. In this case the contraction of the column of liquid begins

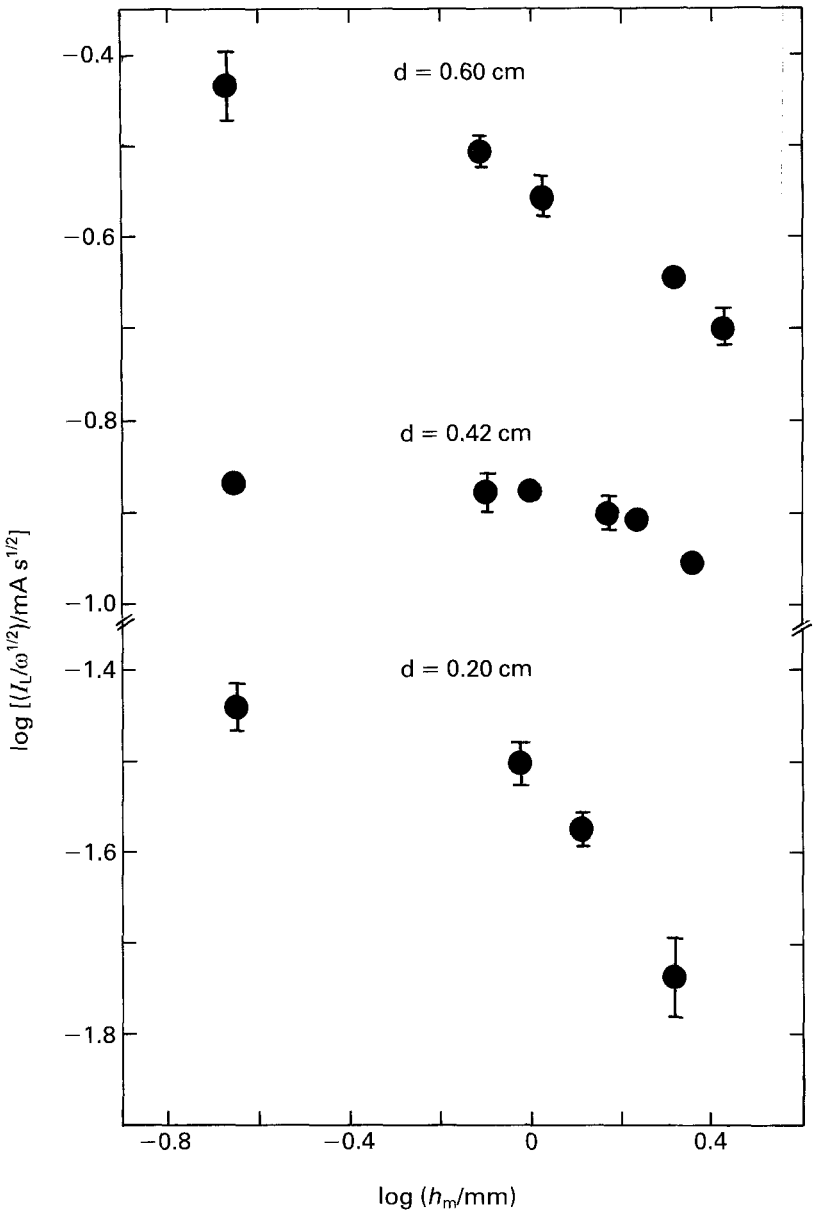

Fig. 4. Logarithmic $I_L/\omega^{1/2}$ ratio against h_m plot for a bare nickel rde at different ω. 0.02 M $K_3[Fe(CN)_6]$ + 0.02 M $K_4[Fe(CN)_6]$ + 1 M NaOH. 25 °C.

to operate as already described for the bare type rdehc. Accordingly, the behaviour is characterized by a decrease in the slope of the I_L against $\omega^{1/2}$ plot. This qualitative interpretation suggests why, when $h_m > h_c$, the behaviour of the I_L against $\omega^{1/2}$ plot for bare and insulating rdehc's becomes similar.

In conclusion, the ionic mass transfer at rdehc reveals the influence of both solution climbing and column height contraction which are reflected in the I_L against $\omega^{1/2}$ linear plots. Thus, the interpretation of such plots for this type of electrode is more complex than for conventional rde's.

5. Conclusions

Ionic mass transport at the rdehc depends considerably on h_m. From the practical standpoint the rdehc can be employed in different ways, such as a bare or an insulated lateral wall electrode, but whatever the case a constant value of h_m is required for comparing electrochemical kinetic data. Furthermore, for quantitative measurements the value of h_m must be adjusted according to the electrode design. Thus, for a bare electrode, the best value of h_m is that which provides $h_L = 0$, so that the effective rdehc area is the geometric area of the disc. Otherwise, for an insulated lateral wall electrode a simple I_L against $\omega^{1/2}$ a straight line relationship emerges when the $h_m = h_c$ condition is fulfilled. The results indicate that a contraction at the hanging electrolyte column is produced, an effect which becomes greater as h_m increases. These facts explain the influence of h_m on the slope of the plots shown in Figs 2 and 3, as the effective electrode surface area changes with h_m.

Acknowledgement

This work was financially supported by the Consejo Nacional de Investigaciones Científicas y Técnicas (CONICET) and the Comisión de Investigaciones

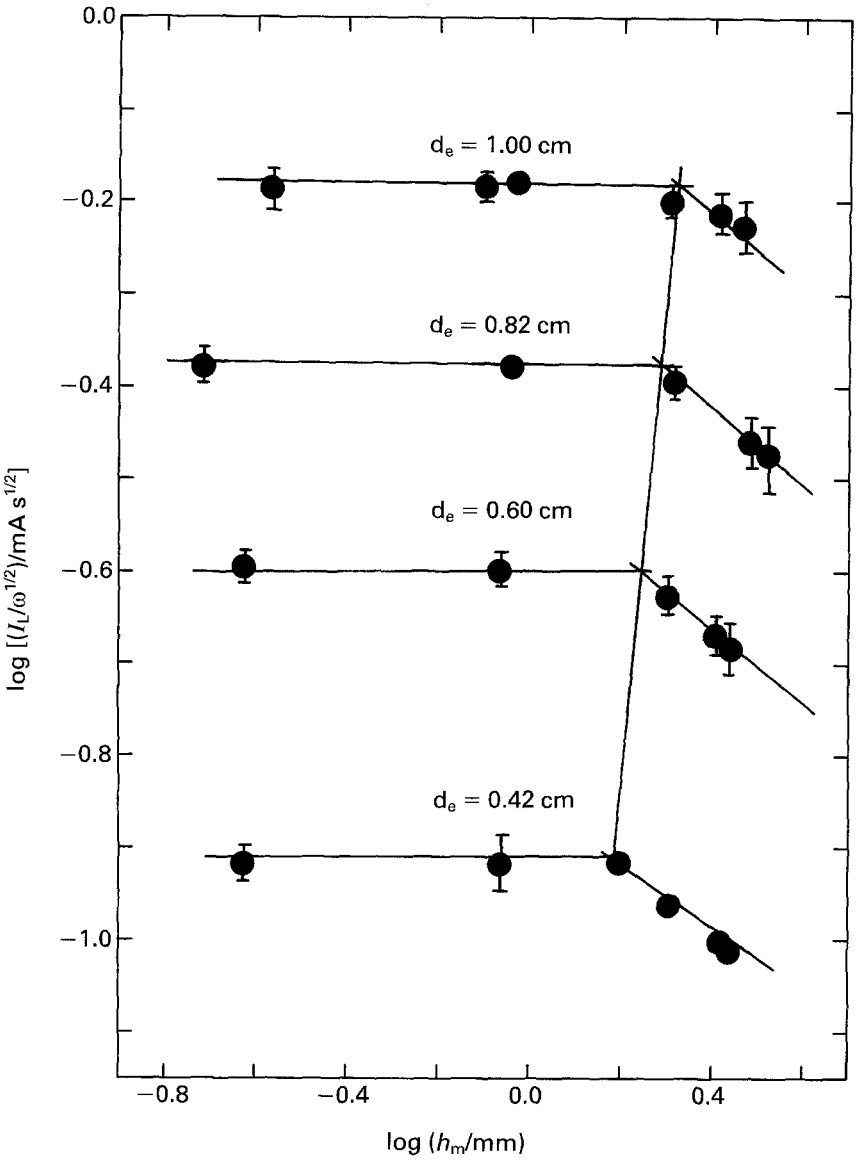

Fig. 5. Logarithmic $I_L/\omega^{1/2}$ ratio against h_m plot for nickel rde with lateral insulation at different ω. 0.02 M $K_3[Fe(CN)_6]$ + 0.02 M $K_4[Fe(CN)_6]$ + 1 M NaOH, 25 °C.

Científicas de la Provincia de Beunos Aires (CIC). P.L. Schilardi thanks CIC, Pcia. Bs.As. for the scholarship granted.

References

[1] V. G. Levich, *Acta Physicochim., URSS* **17** (1942) 257.
[2] *Idem, Zh. Fiz. Khim.* **18** (1944) 335 *Ibid.* **22** (1948) 575.
[3] *Idem*, 'Physicochemical Hydrodynamics', Prentice Hall, Englewood Cliff, NJ (1962).
[4] A. Frumkin and G. Teodoradse, *Z. Elektrochem.* **62** (1958) 251.
[5] A. C. Riddiford, 'Advances in Electrochemistry and Electrochemical Engineering', Vol. 4, Interscience, New York (1966).
[6] Yu. V. Pleskov and V. Yu Filinovskii, 'The Rotating Disc Electrode', Studies in Soviet Science (1976).
[7] W. J. Albery, *Trans. Farad. Soc.* **62** (1966) 1915.
[8] W. J. Albery and S. Bruckenstein, *Trans. Farad. Soc.* **62** (1966) 1920.
[9] A. J. Arvia and S. L. Marchiano, 'Modern Aspects of Electrochemistry', Vol. 6, Chapter 3, Ed. J.O.'M. Bockris and B.E. Conway, Plenum Press, London (1971).
[10] D.-T. Chin, *J. Electrochem. Soc.* **118** (1971) 1434.
[11] O. A. Cobo, S. L. Marchiano and A. J. Arvia, *Electrochim. Acta* **17** (1972) 503.
[12] D. Dickertmann, F. D. Koppitz and J. W. Schultze, *Electrochim. Acta* **21** (1976) 967.
[13] B. D. Cahan and H. M. Villullas, Extended Abstracts Electrochemical Society, **88–2** (1988) 1010–1; *J. Electroanal. Chem.* **307** (1991) 263.
[14] M. M. Laz, R. M. Souto, S. González, R. C. Salvarezza and A. J. Arvia, *Electrochim. Acta* **37** (1992) 655.
[15] R. M. Souto, M. Pérez Sánchez, M. Barrera, S. González, R. C. Salvarezza and A. J. Arvia, *ibid.* **37** (1992) 1437.
[16] D. Gröhne, *Nachr. Akad. Wissenschaf., Göttingen (Math. Phys. Klasse)* **12** (1955) 263.
[17] D. Gröhne, *Z. angew. Math. Mech.* (1956) 2.
[18] J. C. Bazàn and A. J. Arvia, *Electrochim. Acta* **10** (1965) 1025.
[19] A. J. Arvia, S. L. Marchiano and J. J. Podestá, *ibid.* **12** (1967) 259.
[20] A. J. Arvia, J. C. Bazán and J. S. W. Carrozza, *ibid.* **13** (1968) 81.